Theor Chem Acc (2012) 131:1261
DOI 10.1007/s00214-012-1261-4

REGULAR ARTICLE

Ab initio quantum chemical and ReaxFF-based study of the intramolecular iminium–enamine conversion in a proline-catalyzed reaction

Pierre O. Hubin · Denis Jacquemin · Laurence Leherte · Jean-Marie André · Adri C. T. van Duin · Daniel P. Vercauteren

Received: 29 February 2012 / Accepted: 3 July 2012 / Published online: 9 August 2012

Abstract Among all strategies used by organic chemists to control the stereoselectivity of reactions, organocatalysis, which consists in using the chirality of a small organic molecule, is an increasingly popular method. The proline-catalyzed aldol reaction was one of the first reported cases that demonstrated the power of organocatalysis in the field of asymmetric synthesis. Previous theoretical contributions focused on the reaction mechanism using quantum mechanics (QM) methods. We here present a theoretical study about one specific step of the proline-catalyzed aldol reaction, namely, the conversion of the iminium intermediate into the corresponding enamine. It consists of an intramolecular rearrangement that involves the transfer of a hydrogen atom. First, we investigate this transfer using modern QM models, that is, density functional theory calculations with the M06-2X functional. On the basis of these QM results, we then assess the performance of a reactive force field, ReaxFF, used in combination with molecular dynamics simulations in order to provide a complementary light on this reaction.

Keywords ReaxFF · Force field development · Molecular dynamics simulation · Organocatalysis · Reaction pathway · Proline catalysis · Enamine · Iminium · Solvent effects · DFT · M06-2X

Published as part of the special collection of articles celebrating theoretical and computational chemistry in Belgium.

Electronic supplementary material The online version of this article (doi:10.1007/s00214-012-1261-4) contains supplementary material, which is available to authorized users.

P. O. Hubin (✉) · L. Leherte · D. P. Vercauteren (✉)
Laboratoire de Physico-Chimie Informatique, University of Namur, 61, rue de Bruxelles, 5000 Namur, Belgium
e-mail: phubin@student.fundp.ac.be

D. P. Vercauteren
e-mail: daniel.vercauteren@fundp.ac.be

D. Jacquemin
CESIAM UMR CNRS 6230, Université de Nantes, 2, rue de la Houssinière, BP 92208, 44322 Nantes 3, France

J.-M. André
University of Namur, Académie Royale de Belgique, 61, rue de Bruxelles, 5000 Namur, Belgium

A. C. T. van Duin
Department of Mechanical and Nuclear Engineering, Pennsylvania State University, 136 Research East Building, University Park, PA 16802, USA

1 Introduction

The ability to control the stereoselectivity of organic reactions is an important key for experimental chemists. As two enantiomers present the same energy, a source of chirality is required to achieve enantioselective synthesis. An efficient approach to induce the chirality in a product is to take advantage of a chiral catalyst, like enzymes or organometallic compounds [1]. During the last decade, a new class of chiral catalysts has been identified, leading to the emergence of so-called organocatalysis [1–3]. The common characteristic of this class of compounds is not only their composition (carbon, hydrogen, nitrogen, oxygen, or sulfur atoms), but also their relative compactness [1]. A well-known example is (s)-proline that catalyzes asymmetric aldol reactions (Scheme 1) with a large yield as well as with a significant enantiomeric excess [4]. This reaction is indeed one of the first reported cases that demonstrated that a small organic molecule could induce an asymmetric reaction [4]. Other organocatalysts were

later found to be efficient in several reaction paths [1–3, 5–8]. Previous studies, mainly relying on quantum mechanics (QM) techniques, focused on the proline-catalyzed aldol reaction and managed to rationalize the observed selectivity [9–15]. It was proposed that the crucial step to explain the stereoselectivity of the reaction is the C–C bond formation and that the mechanism is controlled mainly by the possibility to form a hydrogen bond and by steric hindrance [9–15]. Even if these studies were quite complete, they lacked information about environment and conformational effects, especially for large molecules. It is due to the relatively large computational cost that QM techniques require. Additionally, the mechanistic questions concerning the proline-catalyzed aldol reaction are still not completely resolved. Though the enamine pathway [9–14] is generally accepted, other explanations partially based on the experimental facts [16–18] propose that oxazolidinone intermediates are likely to occur in the mechanism [17].

Our present contribution is devoted to one of the early step of the proline-catalyzed aldol reaction, namely the conversion of the iminium intermediate formed by proline and an aldehyde into the corresponding enamine (Scheme 1). It corresponds to an intramolecular rearrangement involving the transfer of one hydrogen atom. In this paper, first, a fresh theoretical look at the iminium–enamine conversion is proposed by considering different possible paths for the proton transfer with modern QM techniques and the reactive force field (FF), ReaxFF [19]. This last one is combined with molecular dynamics (MD) simulations to shed a complementary light on several aspects of the reaction. The ReaxFF potential establishes a relation between the bond order and the distance between atoms. Consequently, it is able to handle the breaking and formation of chemical bonds during simulations, allowing thus to investigate chemical reactions. It was originally designed and applied to problems related to hydrocarbons [19], but was subsequently extended to many other families of chemicals [20–23]. For instance, ReaxFF parameters were recently developed to model proton transfer in glycine conformers surrounded by water molecules [23]. Combining a reactive FF with MD simulations to investigate chemical reactions is specifically helpful to take into account effects of the environment. It, instead, still remains a challenge for QM techniques to model explicit solvation due to the large computational cost associated with hundreds of solvent molecules, whereas it is a tractable process in the framework of classical MD simulation.

Our paper is organized as follows. First, we compare the performances of several QM models for mimicking the proton transfer reactions, considering both thermodynamic (relative stabilities of intermediates) and kinetic (values of energetic barriers) parameters. To this end, CCSD(T) [24] energies were computed to obtain reliable benchmarks and to adequately assess the quality of lighter ab initio schemes, notably of several density functional theory (DFT) hybrids. This first step allowed selecting an efficient and accurate QM method to investigate the hydrogen atom transfer in the present framework. In a second stage, we consider different possible conformations for the reagent and the product (Fig. 1), the possibility to have a water-assisted proton transfer, as well as the impact of polar (water and acetonitrile) and apolar (benzene) solvents via QM calculations. Information obtained from ReaxFF MD simulations carried out with explicit water molecules surrounding the reactive species gives insight into the effect of water on the reaction. The selected QM method is also used to estimate the reliability of ReaxFF to model the reaction step framed in Scheme 1.

2 Computational methods

All QM calculations were performed using Gaussian09 [25] aiming at generating an accurate description of the investigated reaction from both thermodynamic and kinetic point of views in order to guide the ReaxFF simulations. Consequently, we concentrated on the definition of a theoretical method which can provide reliable results for the intermediates and the transition states (TS). Four functionals were tested: B3LYP [26], BMK [27], ωB97X-D [28], and M06-2X [29], the former being the *classical* functional used in many simulations of organic reactions, while the three latter are well recognized as more adequate for the investigation of the TS. MP2 [30] geometry optimizations and CCSD(T) single point energy computations on the MP2 structures were also carried out to allow a balanced assessment of the *pros* and *cons* of each functional. Calculations performed to provide comparisons

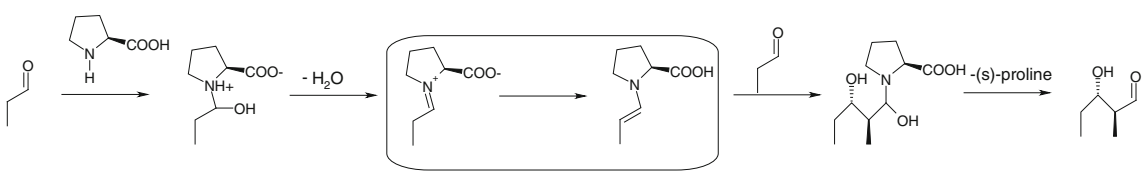

Scheme 1 Representation of the major steps of the proline-catalyzed aldol reaction of propionaldehyde following the enamine pathway [12]. The present contribution focuses on the framed step

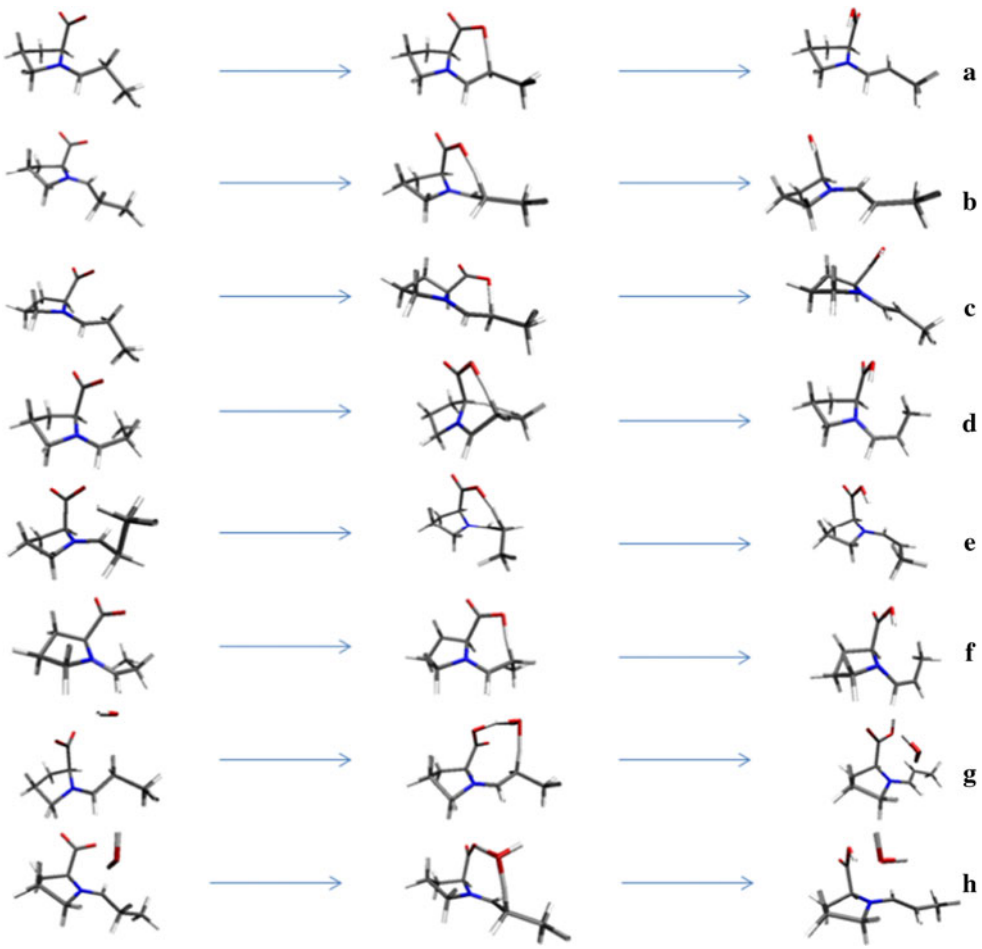

Fig. 1 Sketch of eight conformations of the iminium (*left*) and enamine (*right*) intermediates as well as the transition states (*center*). **a** E *s-cis endo*, **b** E *s-trans endo*, **c** E *s-cis exo*, **d** Z *s-cis endo*, **e** Z *s-trans endo*, **f** Z *s-cis exo*, **g** E *s-cis endo* complexed with one water molecule, and **h** E *s-trans endo* complexed with one water molecule. Carbon, hydrogen, oxygen, and nitrogen atoms are sketched in *gray*, *white*, *red*, and *blue*, respectively. One should notice that the notations regarding the iminium intermediates are defined following the enamine that is formed, for example, iminium E *s-cis endo* being the conformation of iminium leading to the enamine with the E geometry of the double bond, the *s-cis* conformation, and the *endo* conformation of the proline cycle

between the four functionals were done with the 6-311 ++G(d,p) atomic basis set. In the latter steps, the M06-2X/6-31 + G(d,p) scheme was used to investigate several aspects of the reaction as this more compact basis set provided results very similar to its more extended counterpart (see Supplemental Materials Table S2 for a brief comparison of the two basis sets). Vibrational frequencies of all optimized structures were systematically computed to ensure that local minima (no imaginary frequency) or TS (one imaginary frequency) are described. Regarding the TS, the imaginary frequency was checked to correspond to the hydrogen atom transfer between iminium and enamine. The bulk solvent interactions at the QM level were taken into account via the IEF (integral equation formalism)-PCM (polarizable continuum model) method [31].

In the second stage of our work, the program LAMMPS [32] was used to carry out MD simulations of the hydrogen atom transfer in combination with ReaxFF. Before performing simulations of the reaction, we had to assess the performances of the FF for our system. To this end, molecular mechanics (MM) minimizations were done with LAMMPS to compare both geometrical and energetic criteria obtained at the QM and MM levels. Specific FF parameters relevant to the studied reaction were obtained through an optimization process of ReaxFF. The procedure consisted in a single-parameter optimization as described in another contribution [33]. We initially started our investigations with ReaxFF parameters developed for a study regarding the proton transfers in glycine isomers [23]. These parameters were subsequently modified to reproduce QM relative energies related to compounds that include functional groups relevant to our study. MMFF94 [34], another FF for which specific parameters for the iminium and enamine functional groups were already available, was also used with the program Tinker [35] to compare the performances of both FF's.

MD simulations in vacuum were performed in a cubic periodic box of 8,000 $Å^3$ in the canonical NVT ensemble. Tests were also carried out using the microcanonical NVE ensemble but led to large variation of the temperature between the reactant and the product. The temperature was maintained to 100 K with a Nosé-Hoover thermostat [36] so as to limit thermal fluctuation of the energy. As emphasized in a previous study, it indeed appeared that a relatively low temperature was needed to characterize both

intermediates with significant energy values [23]. The iminium intermediate was also put in a box containing solvent molecules to characterize the influence of explicit solvation on the reaction. The number of solvent molecules was fixed to reach the density observed at atmospheric pressure. The temperature for the solvated simulations was also maintained to 100 K. Another important point regarding the simulation of the reaction concerns the triggering of the hydrogen atom transfer. Indeed, while one could in principle expects the reaction to occur spontaneously, this, in practice, can require extremely long simulations to be observed. Consequently, a specific strategy was adopted to trigger the reaction. It consisted in imposing a constraint to force the atoms which are going to form a new bond to come closer. The constraint was set up using the steered-MD function of LAMMPS [37] with a spring constant of 1.0 kcal/mol $Å^2$, sufficient to trigger the reaction within 10 ps for most considered cases. It was not imposed during the whole simulation; a period of equilibration was applied before and after imposing the constraint. The time step was fixed to 0.1 fs when the constraint was acting and to 0.25 fs (in vacuum) or 0.5 fs (with explicit water molecules) otherwise. The choice of a relatively short time step is consistent with the study of chemical reactions involving fast movements of atoms. Especially, we figured out that a 0.1 fs time step was necessary to trigger the reaction without the occurrence of any other undesired event.

3 Results and discussion

3.1 Comparison of QM methods

In this section, we assess the performances of four functionals, B3LYP, BMK, ωB97X-D, and M06-2X, for estimating the relative stabilities of the intermediates and the reaction energy barrier. Benchmarks were obtained with several wavefunction methods using single point energies computed on the MP2 geometries (Table 1). The CCSD(T)/6-311++G(d,p) energy values were in agreement with complete size basis-set extrapolation calculations, that is, CBS/QB3 and G3MP2 approaches, regarding the stability of iminium versus enamine with deviations smaller than 0.6 kcal/mol.

First, it is noticed that MP2 gives values in the line of the CCSD(T) ones. Regarding the four functionals, one sees that BMK and ωB97X-D are particularly efficient for estimating energy barriers but less reliable for predicting the relative stability of the intermediates (errors exceeding 3 kcal/mol). With B3LYP, the energy barrier is also underestimated, an expected outcome for a hybrid functional incorporating a relatively small fraction of *exact* exchange [27, 29, 38, 39]. M06-2X provides very accurate values for intermediates and, though less satisfying for the TS, this *meta*-GGA hybrid functional emerges as adequate for the investigation of the considered reaction. It is indeed the only functional to yield errors smaller than 20 % for both criteria.

Table 1 6-311 ++G(d,p) relative stabilities of the iminium and enamine intermediates and energy barriers associated with the conversion of iminium into enamine for the E *s-cis endo* case, both non-hydrated and water-assisted

QM method	Non-hydrated		Water-assisted	
	Relative stability (kcal/mol)	Energy barrier (kcal/mol)	Relative stability (kcal/mol)	Energy barrier (kcal/mol)
CCSD(T)[a]	14.35	13.20	7.02	22.08
CCSD[a]	15.81 (10.2)	14.23 (7.8)	8.30 (18.2)	24.43 (10.6)
MP4(SDQ)[a]	15.28 (6.5)	13.99 (6.0)	7.79 (11.0)	24.09 (9.1)
MP2	15.00 (4.5)	11.88 (10.0)	7.34 (4.6)	19.15 (13.3)
B3LYP	12.18 (15.1)	10.24 (22.4)	8.27 (17.8)	17.76 (19.6)
BMK	11.19 (22.0)	12.53 (5.1)	5.89 (16.1)	21.93 (0.7)
ωB97XD	10.22 (28.8)	13.78 (4.4)	6.63 (5.6)	19.02 (13.9)
M06-2X	15.13 (5.4)	10.96 (17.0)	8.36 (19.1)	18.05 (18.3)

Zero point vibrational energy (ZPVE) was not taken into account. Relative errors (percentages) with respect to CCSD(T) are given in parentheses

[a] Single point calculation using the MP2 geometry

Among the parameters that influence the reaction, we tested the possibility for a water molecule to mediate the proton transfer. The results reported in Table 1 show the performances of each functional when one single water molecule is complexed with the reactive species.

Though the error of M06-2X for the relative stability is larger, 19.1 %, than for the non-hydrated case, 5.4 %, it remains quite consistent with relative discrepancies below 20 %, an acceptable threshold for our purposes. It is worth highlighting that ωB97X-D performs very well, 5.6 and 13.9 % of errors with respect to CCSD(T), for the water-assisted case, although it was significantly less efficient for the non-hydrated case, 28.8 %, confirming its performances when hydrogen bonds with water molecules play a key role [39]. BMK underestimates the relative energy between the intermediates but it gives a result very close to CCSD(T) for the energy barrier, with an error inferior to 1 %. However, for the non-hydrated case, this functional implies an error superior to 20 % regarding the relative stability.

Combining both non-hydrated and water-assisted cases, one can draw several conclusions. BMK and ωB97X-D behave similarly; they predict energy barriers (especially BMK) rather well but underestimate the relative stability of the intermediates. This error remains limited when the

Table 2 M06-2X/6-31 + G(d,p) relative stabilities and energy barriers for the eight considered cases

	Relative stability (kcal/mol)	Energy barrier (kcal/mol)
E *s-cis endo* (a)	15.14	10.25
E *s-trans endo* (b)	14.77	21.31
E *s-cis exo* (c)	15.88	10.03
Z *s-cis endo* (d)	14.77	11.06
Z *s-trans endo* (e)	11.62	25.80
Z *s-cis exo* (f)	14.94	10.46
E *s-cis endo* + 1 H_2O (g)	13.34	11.91
E *s-trans endo* + 1 H_2O (h)	7.41	16.34

ZPVE corrections were not taken into account. Labels (a)–(h) correspond to those of Fig. 1

absolute value is small but becomes problematic for larger values. B3LYP provides results of average accuracy regarding the relative stability and underrates the energy barriers. M06-2X slightly overestimates the relative stability of the intermediates with an error becoming significant when the absolute value is particularly small. Like B3LYP, it underestimates energy barriers.

In short, we selected the M06-2X functional for all further calculations because it emerges as a suitable compromise for estimating both energy barriers and relative stabilities between intermediates and it is the most consistent method for the two considered cases, non-hydrated and water-assisted. Let us add that the conclusions regarding the selected functional are limited to the case investigated here, and it should not be inferred that it is adequate for any type of reactions.

3.2 Conformational issues

The M06-2X/6-31 + G(d,p) approach was used to investigate conformational aspects of the reaction. Six possible forms of the starting iminium intermediate were considered focusing on three parameters: the conformation of the proline cycle (*endo* or *exo*) [14], the relative position of the methyl group *versus* the carboxylate (*s-cis* or *s-trans*) [15], and the two conformations that may lead to the E or Z configuration of the enamine. Cases (a) to (f) are illustrated in Fig. 1; the results are summarized in Table 2. One should notice that a total of eight cases could have been considered. However, the Z and E *s-trans exo* forms of the iminium were too unstable to be located. The possibility for the hydrogen atom transfer to occur through a water molecule, cases (g) and (h), was also considered (Table 2).

The enamine conformer (b) is of similar stability than its counterpart (a), 0.05 kcal/mol, but the corresponding energy barrier for (b), 21.31 kcal/mol, is far larger than (a), 10.25 kcal/mol. It can be explained by the distance separating the two atoms forming the new bond; the O···H distance is indeed 2.49 Å in iminium (a) but 3.29 Å in iminium (b). We therefore evaluated the possibility to convert enamine (a) into (b). Such a conversion seems energetically allowed: the TS to pass from one form to the other was localized, and the energy barrier associated with this transformation is 6.72 kcal/mol, which is lower than the energy barrier of the reaction, 10.25 kcal/mol. The conformation of the proline cycle, *endo* or *exo*, has a rather negligible impact from both thermodynamic and kinetic points of views. The reaction probably occurs regardless of the starting conformation of the five-membered ring. Comparing cases (a) and (d), the E species are generally favored over the Z ones: the iminium and enamine isomers (a) are more stable than their counterpart (d). The barrier for the formation of the enamines E is also a bit smaller by 0.81 kcal/mol. The difference between (d) and (e) is similar to the one noticed between (a) and (b): the energy barrier associated with the *s-trans* isomer, 25.80 kcal/mol, being much larger than the one of the *s-cis* one, 11.06 kcal/mol.

The sizeable energy barriers in the *s-trans* cases are related to the distances between the oxygen and the hydrogen atoms, and they can be potentially decreased if a water molecule assists the transfer of the hydrogen. This scenario was investigated by comparing the energy barriers of the water-assisted transfer for the E *endo s-cis* (g) and E *endo s-trans* (h) structures. The corresponding TS may be viewed in Fig. 1. The results shown in Table 2 indicate that the hypothesis is verified: the energy barrier is decreased by 4.97 kcal/mol for the *s-trans* case and slightly increased for the *s-cis* one, 1.66 kcal/mol. This is consistent with previously published data [15].

Our conclusion is thus that the transfer is more likely to happen from the E *s-cis endo* form of the iminium to yield the enamine E *s-cis endo*, which is probably in equilibrium with the E *s-trans endo* one.

As mentioned in the introduction, there is an alternative mechanistic pathway supporting that the iminium–enamine conversion occurs through an oxazolidinone intermediate. We tested the possibility to form oxazolidinone from the E *endo s-trans* isomer of the iminium. It turns out that the energy barrier for this conversion is very low, 0.20 kcal/mol. Moreover, this oxazolidinone species is more stable than the other considered intermediates, the difference being 7.44 kcal/mol regarding the enamine E *endo s-trans*. These results are not particularly surprising since, on the one hand, it is known from experimental observations that oxazolidinones are easily isolated in the reaction mixture, although it is nearly never the case for enamines, and, as on the other hand, similar theoretical results were already

reported in literature. Nevertheless, the oxazolidinone formed must be subsequently opened to yield a negatively charged enamine and no element proves that this particular step is kinetically favored over the direct iminium–enamine conversion, especially if no base is added in the reaction mixture to allow the elimination process. Sharma et al. [15] investigated the possibility for the oxazolidinone opening to occur in presence of trimethylamine and found a Gibbs free energy of activation of 18.0 kcal/mol with the B3LYP functional. As far as we are concerned, those values of energy barriers are too close to completely rule out one or another pathway which may also vary following the reaction conditions.

To this point, we did not take into account entropic effects. A summary of the influence of these contributions is given in "Supplemental Materials." Globally, the enthalpic contribution is clearly predominant from both thermodynamic and kinetic point of views, an expected outcome for an intramolecular reaction. Consequently, for the rest of the work, only enthalpic contributions are considered, these ones being directly comparable with the FF potential energies.

Table 3 M06-2X/6-31 + G(d,p) relative stabilities between the two intermediates and energy barriers for the case E *s-cis endo* considering several solvent models

	Relative stability (kcal/mol)	Energy barrier (kcal/mol)
1: Vacuum	15.14	10.25
2: Implicit solvation, single point energy (IEF-PCM, CH_3CN)	2.37	15.37
3: Implicit solvation, geometry optimization (IEF-PCM, CH_3CN)[a]	0.31	18.13
4: Implicit solvation, geometry optimization (IEF-PCM, water)	−5.56	18.82
5: Five explicit water molecules + implicit solvation (IEF-PCM, water)[b]	−7.57	24.48

ZPVE corrections were not taken into account

[a] The enamine conformation considered in 1, 2, and 3 is not the same than in 4 and 5

[b] The geometries of the solutes are the ones optimized in 4

3.3 Solvation effects

Experimentally, the low solubility of proline in common organic solvents is a problem for the proline-catalyzed aldol reaction [40]. The problem can be circumvented by using polar aprotic solvents like DMSO [4]. Water can also be used as co-solvent; it speeds up the reaction and allows using only stoichiometric quantities of ketones [40]. The reaction still works when performed in water with no other co-solvent, but to the price of a loss of selectivity [40].

To model bulk effects of solvents such as acetonitrile and water, we used the IEF-PCM algorithm. First, single points were computed on the vacuum geometries. The second step consisted in optimizing the geometries of the structures under implicit solvation. A summary of the different approaches and results for the E *s-cis endo* case is presented in Table 3.

The global trend can be summarized as follows: the more the description of the solvent is complete, the more the iminium intermediate is stabilized with respect to the enamine and the TS. In terms of implicit solvation, the last observation is easily understood since the stabilizing effect of polar solvents is larger for polar solutes. The dipole moment of iminium in vacuum computed at the M06-2X/6-31 + G(d,p) level is indeed 9.94 D, which is 1.52 (4.49) D larger than the TS (enamine) dipole moment. This implies that the energy barrier in polar solvents is increased with respect to vacuum [12, 41]. Similarly, the relative stability of iminium *versus* enamine is shifted in favor of the former, the effect being larger when the geometry optimization is carried out with implicit solvation.

To model explicit solvation, single point energies were computed on systems composed of solute molecules (whose geometries were optimized at the M06-2X/6-31 + G(d,p) level with implicit solvation) surrounded by five molecules of water, the rest of the solvent being treated implicitly. To set up the position of the solvent molecules, we relied on MD simulations carried out with ReaxFF with explicit solvent molecules. However, five water molecules are not sufficient to completely describe the first solvation shell. For this reason, the positions of the water molecules were adjusted to ensure the comparison of similar situations for iminium, enamine, and the TS. Let us precise that in this case the solvent molecules do not play an active role in the reaction (they do not mediate the hydrogen atom transfer) but may stabilize one intermediate over the other and tune the height of the barrier. The explicit water molecules stabilize even more the iminium intermediate, which becomes more stable than the enamine by 7.57 kcal/mol. In addition, the energy barrier is raised by 5.56 kcal/mol. This outcome suggests that using only implicit solvation yields an underestimation of the stability of iminium. This additional stabilization of iminium originates in the strong hydrogen bonds between the carboxylate group and water molecules. This observation is consistent with what can be deduced from the ReaxFF MD simulations of the reaction. Following the evolution of the system composed by the iminium intermediate surrounded by 104 molecules of water, it is seen that both oxygen atoms of the carboxylate are close to hydrogen atoms of water.

The mean distances computed during the simulation are 1.67 ± 0.07 and 1.64 ± 0.04 Å. These short distances suggest an interaction stronger than a simple H-bond, and it is consistent with the raise of the barrier of the reaction. The hydrogen atom transfer is indeed less likely to occur when the oxygen of the carboxylate is involved in a strong interaction with water molecules.

3.4 Validation of the FF

To evaluate the performances of ReaxFF for the reaction, we compare the reference QM results, obtained with the M06-2X functional and the 6-31 + G(d,p) basis set, with MM geometry optimizations and single point energy calculations. When it is possible, we also compare these results with MMFF94 data [34], another FF that contains specific parameters for the iminium and enamine functional groups.

Our first criterion to evaluate ReaxFF is the energy. We compare relative energies between several intermediates of the reaction obtained from the optimized QM and FF geometries. Selected results are presented in Table 4, the five top lines correspond to relative energies of selected isomers, for example, E *s-cis endo versus* E *s-trans endo*, whereas the bottom three lines imply different molecules. For the first category, ReaxFF performances are quite similar to MMFF94 ones: MMFF94 is slightly better for the comparison of the enamine E *s-cis endo* (a) and Z *s-cis endo* (d), but it was impossible to locate two different conformations for the iminium conformers (a) and (d) with MMFF94. Actually, the geometry optimization systematically yields the conformer (a), regardless of the starting point.

MMFF94 cannot be used to compare the structural isomers as it does not grant meaningful comparison between molecules with different connectivities. The computed energy indeed depends on the atom types that change between iminium and enamine. ReaxFF is able to qualitatively reproduce QM results: the enamine intermediates remain more stable than iminium ones, though the difference is slightly overestimated by ReaxFF.

Table 4 Relative energies (in kcal/mol) of optimized structures of several intermediates with different QM (M06-2X/6-31 + G(d,p) and FF (ReaxFF and MMFF94) methods

Structures[a]	M06-2X	ReaxFF	MMFF94
Enamine (b)/(a)[b]	−0.05	0.03	0.59
Iminium (b)/(a)	−0.42	−0.13	0.37
Enamine (d)/(a)	2.09	6.02	3.63
Iminium (d)/(a)	1.71	3.44	0.00
Enamine (h)/(g)	0.63	−3.82	−6.09
Iminium (a)/enamine (a)	15.14	19.52	–
Iminium (d)/enamine (d)	14.77	16.94	–
Iminium (g)/enamine (g)	13.34	16.10	–

[a] Relative energies are computed by subtracting the energy of the second structure to the first

[b] Labels (a)–(h) refer to cases presented in Fig. 1

For the water-assisted cases, one notes that the structure of the enamine E *s-trans endo* (h) optimized with ReaxFF is close to the QM structure, but it is not the case with MMFF94, the water molecule in the optimized geometry departing from its initial position (*cfr* Supplemental Materials). This explains the large error, 6.72 kcal/mol, observed for MMFF94 in that case.

In short, from these data one can conclude that ReaxFF provides results that are comparable to those obtained with MMFF94 for conformers. In general, ReaxFF is able to satisfactorily reproduce QM predictions.

Turning toward the performances of ReaxFF to describe structures perturbed by variations of bond lengths, valence angles, and torsion angles, we compared four potential energy curves as presented in Fig. 2 for key structural parameters (*cfr* Fig. 3 for atom labels). We selected the following strategy: starting from the equilibrium geometry of the QM level of reference, we progressively modified a geometrical parameter and computed QM and ReaxFF single point energies on the obtained structures.

Both bonds are particularly interesting since one is broken, C1-H24, and the other is formed, O15-H24, during the reaction. One notes that ReaxFF reproduces well the bond stretching energies. There is a deviation when the bond lengths are constrained to very small values, for example, 0.7 Å. However, this is not problematic since such situation does not take place in actual chemical reactions. One can also notice that the equilibrium values of the bond lengths are well reproduced by the FF.

As for bond lengths, the position of the minimum for the C20-C1-H24 valence angle is well reproduced by the FF. The curvature is also similar for large angles. For small angles, however, ReaxFF energies are significantly overestimated. To explain this discrepancy, one must refer to the form of ReaxFF. As bond orders are calculated on the basis of distances between atoms, it must prevent the atoms from being involved in more bonds than expected. Thus, an overcoordination penalty term is present in the FF. If one focuses on the geometry of the iminium when the C20-C1-H24 valence angle is constrained to 60° (Fig. 4), one sees that the hydrogen atom H24 is simultaneously close, with distances lower than 1.4 Å, to two carbon atoms, C1 and C20. It follows that H24 and C20 are largely overcoordinated, and thus the overcoordination penalty becomes very large, around 90 kcal/mol. To show that the deviation from QM results is not due to the valence angle description of ReaxFF, we plotted the valence angle energy term in function of the C20-C1-H24 angle (Fig. 4) and the MM *versus* QM discrepancy diminishes.

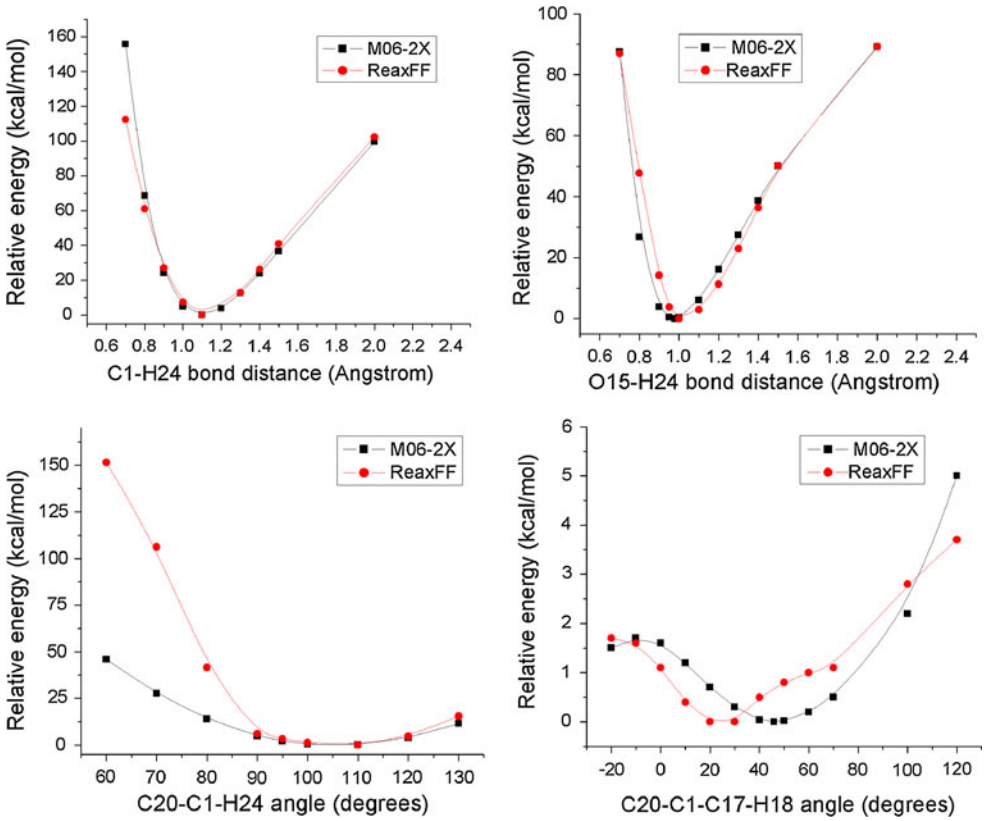

Fig. 2 Relative energy versus the C1-H24 bond length in iminium E s-*cis endo* (*top left*), the O15-H24 bond length in enamine E *s-cis endo* (*top right*), the C20-C1-H24 valence angle (*bottom left*), and the C20-C1-C17-H18 torsion angle (*bottom right*) in iminium E s-*cis endo* as obtained at the M06-2X/6-31 + G(d,p) level and with ReaxFF. Labels of the atoms are given in Fig. 3

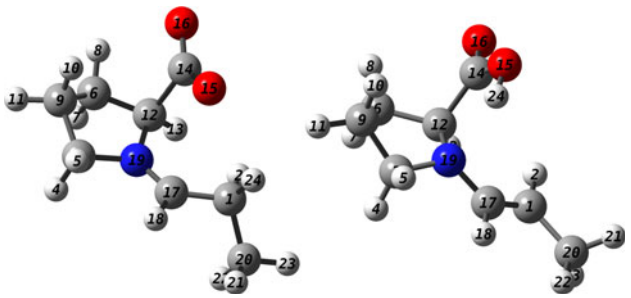

Fig. 3 Sketch of the iminium (*left*) and enamine (*right*) E *s-cis endo* 3D structures with labeled atoms. Colors of the atoms are given in Fig. 1

For the C20-C1-C17-H18 torsion angle in iminium, one notes that the position of the minimum is shifted to smaller angles, 20°, with respect to the QM equilibrium value, 45°. However, the energy difference between these conformations is quite small, that is, less than 2 kcal/mol in the range −20–70°. This small value indicates that the torsion angle is likely to vary significantly during simulations (*cfr* Sect. 3.5).

One can conclude that QM results are reasonably reproduced by ReaxFF. Consequently, one can be confident to find reliable results regarding the investigated reaction with the MD simulations of the hydrogen atom transfer, as described below.

3.5 ReaxFF MD simulations

Let us now focus on the results of the ReaxFF MD simulations. As mentioned in Sect. 2, a constraint was applied on the system to trigger the reaction. The evolution with time of the C···H and H···O distances throughout the simulation is presented in Fig. 5. The C···H distance first fluctuates around a value of 1.1 Å, which corresponds to a C–H σ-bond. After the reaction (34 ps), the distance varies on a larger range since the atoms are not bonded anymore in the enamine structure. The H···O distance decreases gradually before the hydrogen atom is transferred, a direct consequence of the constraint. Once the transfer is triggered, the reaction happens on a very short time scale (about 0.25 ps). This makes the characterization of the TS less straightforward. The solution adopted to tackle the problem was to select an atomic configuration characteristic of the TS and perform a new MD simulation with this configuration as starting point after having fixed the

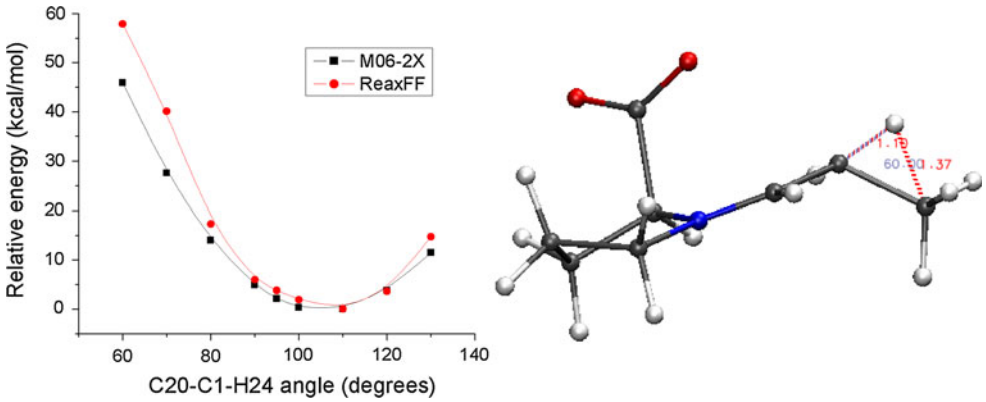

Fig. 4 Comparison between the total QM energy and the valence angle ReaxFF energy contribution for different values of the C20-C1-H24 valence angle in iminium E *s-cis endo*. The structure when the angle is constrained to 60.0° is illustrated on the *right*. Colors and labels of the atoms are given in Figs. 1 and 3, respectively

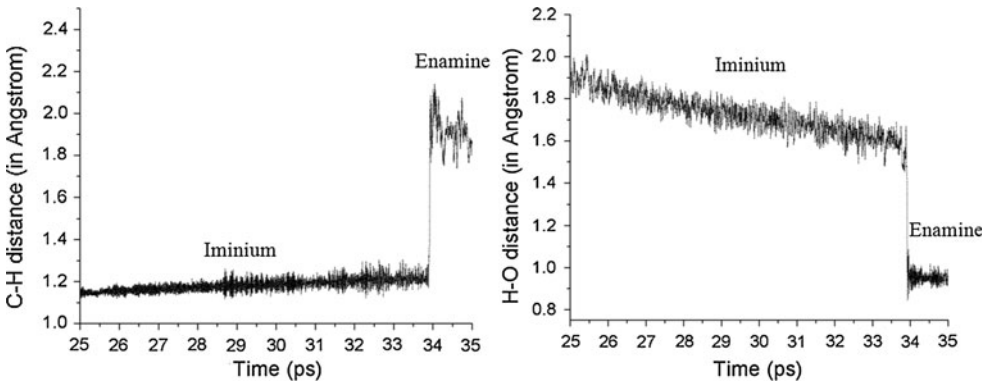

Fig. 5 Evolution of C···H (*left-broken bond*) and H···O (*right-formed bond*) distances during the ReaxFF MD simulation of the conversion of iminium E *s-cis endo* into the corresponding enamine at a temperature of 100 K (NVT ensemble) in vacuum

positions of the three atoms directly involved in the hydrogen atom transfer, that is, C1, H24, and O15.

A summary of the relative stabilities and energy barriers obtained with the M06-2X/6-31 + G(d,p) scheme (*cfr* Table 2) as well as deduced from the MD simulations in vacuum carried out using ReaxFF is presented in Table 5. The energy values of the intermediates from the MD simulations were determined by averaging the potential energies over a time range of 5 ps. For the TS, energies were evaluated on the basis of simulations in which the positions of the atoms involved in the hydrogen atom transfer were held fixed. Errors on the potential energies estimated via the standard deviations stay between 1.0 and 1.5 kcal/mol. Let us mention that we here considered potential energy values obtained from the simulations carried out in vacuum because they can be directly compared to QM energies (without any ZPVE, neither thermal, nor entropic corrections). Explicit solvation effects deduced from simulations cannot be easily related to implicit QM ones, due to the huge difference between the considered systems. Moreover, the parameterization of ReaxFF for this study was performed on the basis of QM results obtained in vacuum, without implicit solvation data. All those reasons explain why the simulations in vacuum are taken into account at this point to compare QM and MD simulations results. Let us also emphasize that it is much easier to extract relative stabilities between intermediates and energy barriers from simulations in vacuum; standard deviations associated with the mean values of potential energies being indeed much larger when considering simulations carried out in a box of water molecules.

From Table 5, it is seen that ReaxFF overshoots the stability of enamine with errors in the range 2.5–4.0 kcal/mol. ReaxFF also slightly overestimates energy barriers,

Table 5 Relative stabilities between the iminium and enamine intermediates and energy barriers associated with the conversion of iminium into enamine in six cases as obtained with the M06-2X/6-31 + G(d,p) scheme and as deduced from the ReaxFF MD simulations at a temperature of 100 K (NVT ensemble) in vacuum

	M06-2X		ReaxFF	
	Relative stability (kcal/mol)	Energy barrier (kcal/mol)	Relative stability (kcal/mol)	Energy barrier (kcal/mol)
E *s-cis endo*	15.14	10.25	18.4	11.2
E *s-trans endo*	14.77	21.31	17.7	27.2
E *s-cis exo*	15.88	10.03	20.0	12.9
Z *s-cis endo*	14.77	11.06	17.5	13.0
Z *s-trans endo*	11.62	25.80	15.7	31.0
Z *s-cis exo*	14.94	10.46	17.2	11.5

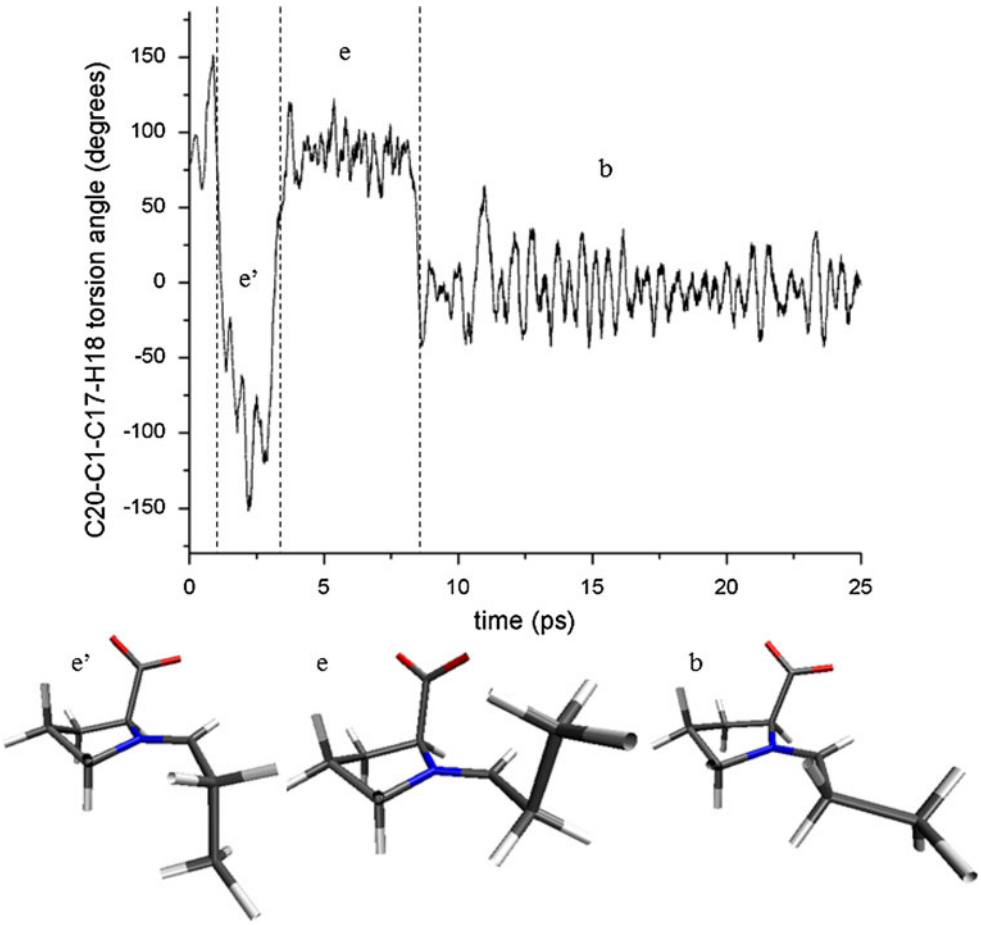

Fig. 6 Evolution of the C20-C1-C17-H18 torsion angle value of the iminium Z *s-trans endo* during the ReaxFF MD simulation performed at 100 K (NVT ensemble) in vacuum. The three conformations, (*e'*), (*e*), and (*b*), encountered during the simulation are illustrated below, labels correspond to the ones given in Fig. 1. Colors and labels of the atoms are given in Figs. 1 and 3, respectively

that is, between 1 and 3 kcal/mol for the *s-cis* cases, for which M06-2X energy barriers are predicted around 10 kcal/mol. The overestimation is slightly larger, around 5 kcal/mol, for the *s-trans* cases, which are predicted around 20–25 kcal/mol with the QM method. ReaxFF results can also be compared to CCSD(T) benchmarks: in the E *s-cis* case, the overestimation using ReaxFF is 4.0 kcal/mol for the relative stability between intermediates and 2.0 kcal/mol regarding the energy barrier. For *s-cis* isomers, it is clear, on the basis of the computed standard deviations, 1.0–1.5 kcal/mol, that ReaxFF cannot precisely indicate whether the hydrogen atom transfer takes place from one specific conformer of the iminium intermediate. Nevertheless, ReaxFF reproduces correctly the much higher energy barriers needed to initiate the hydrogen atom transfer from the *s-trans* forms.

As mentioned in Sect. 3.4, the C20-C1-C17-H18 torsion angle in iminium is relatively flexible. This statement concerned the iminium E *s-cis endo*. From Fig. 6, one sees that this torsion angle in the iminium Z *s-trans endo* is indeed very flexible; three main conformations are observed during the ReaxFF MD simulation. The last one, the most significant if the times passed in each conformation are compared, does not correspond to the Z *s-trans endo* iminium but rather to the E *s-trans endo* (Fig. 6). A much longer simulation of 400 ps was also carried out confirming that the major conformation of iminium was E. The same behavior was observed for the Z *s-cis exo* iminium that had the tendency to switch to the E conformation during the simulation. It is particularly interesting since energy barriers for the *s-cis* isomers are too close to conclude that one is kinetically favored over the other. This switch between E and Z conformations constitutes a thermodynamic argument, showing that iminium is more likely to adopt an E conformation and can thus be converted into E configurations of the enamine.

4 Conclusions

Our theoretical investigation regarding the understanding of the conversion of iminium into enamine in the framework of a proline-catalyzed aldol reaction emphasizes that the reactive force field (FF), ReaxFF, used in combination with molecular dynamics (MD) simulations is a relevant method to investigate the mechanism of proton transfers in iminium–enamine conversions. This approach should be extended to model other steps of proline-catalyzed

reactions. ReaxFF simulations allow investigating the evolution of the system in time, which is useful to assess the likelihood of a given conformational change. Combining MD simulations with explicit inclusion of the solvent is a powerful tool to rationalize the interactions it may form with the solute.

First, we showed that similar conclusions regarding the relative stability of intermediates and energy barriers could be drawn either from ReaxFF MD simulations or from DFT calculations at the M06-2X/6-31 + G(d,p) level. Regarding the particular studied step of the reaction, one showed that the iminium–enamine conversion is more likely to yield an E enamine and that the energy barrier for the reaction is also smaller starting from the *s-cis* isomer of iminium relatively to the *s-trans* one.

We now plan to investigate other steps of the reaction. Particularly, we will focus on the possibility to form the enamine through the opening of the oxazolidinone intermediate. The C–C bond formation step, which is significant to explain the stereoselectivity of the proline-catalyzed aldol reaction, will also be considered. The modeling of other solvents is another perspective for future work.

Acknowledgments The authors acknowledge the support of the F.R.S.-FRFC (convention no. 2.4.617.07.F), and the "Facultés Universitaires Notre-Dame de la Paix" (FUNDP) for the use of the Interuniversity Scientific Computing Facility (ISCF) Center. They are also thankful to Prof. S. Lanners (FUNDP) for fruitful discussions. DJ indebted to the *Régions des Pays de Loire (recrutement sur poste stratégique)* and to the ERC StG program (Grant: Marches–278845) for financial support.

References

1. MacMillan DWC (2008) Nature 455:304–308
2. Dalko PI, Moisan L (2004) Angew Chem Int Ed 43:5138–5175
3. Geary LM, Hultin PG (2009) Tetrahedron Asymmetry 20: 131–173
4. List B, Lerner RA, Barbas CF III (2000) J Am Chem Soc 122:2395–2396
5. Doyle AG, Jacobsen EN (2007) Chem Rev 107:5713–5743
6. Ouellet SG, Tuttle JB, MacMillan DWC (2005) J Am Chem Soc 127:32–33
7. Reisman SE, Doyle AG, Jacobsen EN (2008) J Am Chem Soc 130:7198–7199
8. Yang HY, Hong JB, MacMillan DWC (2007) J Am Chem Soc 129:7004–7005
9. Bahmanyar S, Houk KN (2001) J Am Chem Soc 123: 11273–11283
10. Bahmanyar S, Houk KN (2001) J Am Chem Soc 123: 12911–12912
11. Bahmanyar S, Houk KN, Martin HJ, List B (2003) J Am Chem Soc 125:2475–2479
12. Allemann C, Gordillo R, Clemente FR, Cheong PH-Y, Houk KN (2004) Acc Chem Res 37:558–569
13. Clemente FR, Houk KN (2005) J Am Chem Soc 127: 11294–11302
14. Allemann C, Um JM, Houk KN (2010) J Mol Catal A 324:31–38
15. Sharma AK, Sunoj RB (2010) Angew Chem Int Ed 49:6373–6377
16. Klussmann M, Iwamura H, Mathew SP, Wells DH Jr, Pandya U, Armstrong A, Blackmond DG (2006) Nature 441:621–623
17. Seebach D, Beck AK, Badine DM, Limbach M, Eschenmoser A, Treasurywala AM, Hobi R (2007) Helv Chim Acta 90:425–471
18. Kanzian T, Lakhdar S, Mayr H (2010) Angew Chem Int Ed 49:9526–9529
19. van Duin ACT, Dasgupta S, Lorant F, Goddard WA III (2001) J Phys Chem A 105:9396–9409
20. Chenoweth K, Cheung S, van Duin ACT, Goddard WA III, Kober EM (2005) J Am Chem Soc 127:7192–7202
21. Chenoweth K, van Duin ACT, Goddard WA III (2008) J Phys Chem A 112:1040–1053
22. Zhang L, Zybin SV, van Duin ACT, Dasgupta S, Goddard WA III, Kober EM (2009) J Phys Chem B 113:10619–10640
23. Rahaman O, van Duin ACT, Goddard WA III, Doren DJ (2011) J Phys Chem B 115:249–261
24. Raghavachari K, Trucks GW, Pople JA, Head-Gordon M (1989) Chem Phys Lett 157:479–483
25. Gaussian 09, Revision B01, Frisch MJ, Trucks GW, Schlegel HB, Scuseria GE, Robb MA, Cheeseman JR, Scalmani G, Barone V, Mennucci B, Petersson GA, Nakatsuji H, Caricato M, Li X, Hratchian HP, Izmaylov AF, Bloino J, Zheng G, Sonnenberg JL, Hada M, Ehara M, Toyota K, Fukuda R, Hasegawa J, Ishida M, Nakajima T, Honda Y, Kitao O, Nakai H, Vreven T, Montgomery, Jr JA, Peralta JE, Ogliaro F, Bearpark M, Heyd JJ, Brothers E, Kudin KN, Staroverov VN, Kobayashi R, Normand J, Raghavachari K, Rendell A, Burant JC, Iyengar SS, Tomasi J, Cossi M, Rega N, Millam JM, Klene M, Knox JE, Cross JB, Bakken V, Adamo C, Jaramillo J, Gomperts R, Stratmann RE, Yazyev O, Austin AJ, Cammi R, Pomelli C, Ochterski JW, Martin RL, Morokuma K, Zakrzewski VG, Voth GA, Salvador P, Dannenberg JJ, Dapprich S, Daniels AD, Farkas Ö, Foresman JB, Ortiz JV, Cioslowski J, Fox DJ, Gaussian, Inc, Wallingford CT, 2010
26. Becke AD (1993) J Chem Phys 98:1372–1377
27. Boese AD, Martin JML (2004) J Chem Phys 121:3405–3416
28. Chai JD, Head-Gordon M (2008) Phys Chem Chem Phys 10:6615–6620
29. Zhao Y, Truhlar DG (2008) Theor Chem Acc 120:215–241
30. Møller C, Plesset MS (1934) Phys Rev 46:618–622
31. Tomasi J, Mennucci B, Cammi R (2005) Chem Rev 105:2099–3093
32. Plimpton SJ (1995) J Comp Phys 117:1–19
33. van Duin ACT, Baas JMA, van de Graaf B (1994) J Chem Soc, Faraday Trans 90:2881–2895
34. Halgren TA (1996) J Comp Chem 17:490–519
35. Ponder J (2011) Tinker 5.1.09, program available on: http://dasher.wustl.edu/tinker/. Last consulted on 2 December 2011
36. Shinoda W, DeVane R, Klein ML (2007) Mol Sim 33:27–36
37. Izrailev S, Stepaniants S, Isralewitz B, Kosztin D, Lu H, Molnar F, Wriggers W, Schulten K (1998) Computational molecular dynamics: challenges, methods, ideas. In: Deuflhard P, Hermans J, Leimkuhler B, Mark AE, Reich S, Skeel RD (eds) Lecture notes in computational science and engineering, vol 4. Springer, Berlin, pp 39–65
38. Wodrich MD, Corminboeuf C, Schleyer PVR (2006) Org Lett 8:3631–3634
39. Burns LA, Vazquez-Mayagoitia A, Sumpter BG, Sherrill CD (2011) J Chem Phys 134:84107–84114
40. Pihko PM, Laurikainen KM, Usano A, Nyberg AI, Kaavi JA (2006) Tetrahedron 62:317–328
41. Rankin KN, Gauld JW, Boyd RJ (2002) J Phys Chem A 106:5155–5159